Advance Publication

Circulation Journal
doi:10.1253/circj.CJ-24-0630

ORIGINAL ARTICLE

Predicting Short-Term Mortality in Patients With Acute Pulmonary Embolism With Deep Learning

Vedat Cicek, MD; Ahmet Lutfullah Orhan, MD; Faysal Saylik, MD; Vanshali Sharma, PhD; Yalcin Tur; Almina Erdem, MD; Mert Babaoglu, MD; Omer Ayten, MD; Solen Taslicukur, MD; Ahmet Oz, MD; Mehmet Uzun, MD; Nurgul Keser, MD; Mert Ilker Hayiroglu, MD; Tufan Cinar, MD; Ulas Bagci, PhD

Background: Accurate prediction of short-term mortality in patients with acute pulmonary embolism (PE) is critical for optimizing treatment strategies and improving patient outcomes. The Pulmonary Embolism Severity Index (PESI) is the current reference score used for this purpose, but it has limitations regarding predictive accuracy. Our aim was to develop a new short-term mortality prediction model for PE patients based on deep learning (DL) with multimodal data, including imaging and clinical/demographic data.

Methods and Results: We developed a novel multimodal deep learning (mmDL) model using contrast-enhanced multidetector computed tomography scans combined with clinical and demographic data to predict short-term mortality in patients with acute PE. We benchmarked various machine learning architectures, including XGBoost, convolutional neural networks (CNNs), and Transformers. Our cohort included 207 acute PE patients, of whom 53 died during their hospital stay. The mmDL model achieved an area under the receiver operating characteristic curve (AUC) of 0.98 (P<0.001), significantly outperforming the PESI score, which had an AUC of 0.86 (P<0.001). Statistical analysis confirmed that the mmDL model was superior to PESI in predicting short-term mortality (P<0.001).

Conclusions: Our proposed mmDL model predicts short-term mortality in patients with acute PE with high accuracy and significantly outperforms the current standard PESI score.

Key Words: Deep learning; Pulmonary embolism; Pulmonary Embolism Severity Index (PESI); Short-term mortality

Acute pulmonary embolism (PE) is a severe and sometimes fatal condition caused by a blockage in one or more pulmonary arteries, usually due to a blood clot that forms in the veins of the legs or pelvis.[1,2] This blockage can disrupt blood flow and increase pressure in the right ventricle (RV). PE is a leading cause of death in hospitals, ranked just behind myocardial infarction and stroke.[3] In the US, PE is believed to result in around 100,000 deaths each year,[4] costing the healthcare system between USD7 and 10 billion annually.[5]

The short-term (within 0–30 days) mortality rate of PE varies between 5% and 15%, and is influenced by various factors. Shock or ongoing hypotension indicates a subgroup of PE patients who are at a high risk of mortality. Numerous randomized controlled trials have reported several risks factors for PE that can be used as potential markers for early complications or short-term mortality.[6] Distinguishing between low- and high-risk patients in PE is important for determining the treatment approach and estimating prognosis.[7,8] To this end, several prognostic classifications have been developed for PE patients. The most commonly used prognostic method is the Pulmonary Embolism Severity Index (PESI), designed by Aujesky et al. in 2005, which is recommended by international guidelines.[9] The PESI incorporates 11 clinical variables, including demographic characteristics, such as the presence of

Received August 12, 2024; revised manuscript received October 21, 2024; accepted October 29, 2024; J-STAGE Advance Publication released online November 30, 2024 Time for primary review: 13 days

Machine & Hybrid Intelligence Lab, Department of Radiology, Northwestern University, Chicago, IL (V.C., V.S., U.B.), USA; Sultan II Abdülhamid Han Training and Research Hospital, Department of Cardiology (A.L.O., A.E., M.B., M.U., N.K.), Sultan II Abdülhamid Han Training and Research Hospital, Department of Pulmonary Medicine (O.A.), Health Sciences University, Istanbul; Van Training and Research Hospital, Department of Cardiology, Health Sciences University, Van (F.S.), Turkey; Department of Computer Science, Stanford University, Stanford, CA (Y.T.), USA; Department of Cardiology, Istanbul Education and Research Hospital, Istanbul (S.T., A.O.); Department of Cardiology, Dr. Siyami Ersek Cardiovascular and Thoracic Surgery Research and Training Hospital, Istanbul (M.I.H.), Turkey; and Department of Medicine, University of Maryland, Baltimore, MD (T.C.), USA

Mailing address: Vedat Cicek, MD, Machine & Hybrid Intelligence Lab, Department of Radiology, Northwestern University, 737 N. Michigan Avenue Suite 1600, Chicago, IL 60611, USA. email: Vedat.cicek@northwestern.edu

All rights are reserved to the Japanese Circulation Society. For permissions, please email: cj@j-circ.or.jp

ISSN-1346-9843

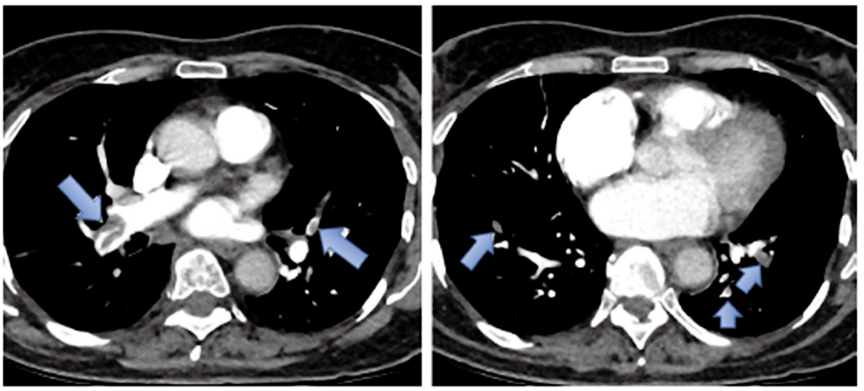


Figure 1. Representative images of lobar (**Left**) and subsegmental (**Right**) pulmonary embolism. Arrows indicate embolic materials (thrombosis).

heart failure and a history of cancer, as well as vital signs, such as hypotension and tachycardia.[10] Although the sensitivity of the PESI score is relatively high (80–90%), its specificity is quite low (40–60%).[11] Therefore, more useful prediction models are needed for the prognosis of patients with PE. These studies have yielded valuable insights into the short-term prognosis of acute PE patients by identifying a combination of clinical, biomarker, and imaging markers. The integration of these factors into a novel risk model empowers early and accurate prediction of prognostic trajectories, facilitating timely and effective treatment interventions.

The aim of the present study was to develop a multimodal deep learning (mmDL) model incorporating results of computed tomography (CT) scans and clinical/demographic data to predict short-term (0–30 day) mortality in PE patients. We aimed to develop a model with superior performance to the current reference standard, PESI.

Methods

Study Population

Acute PE is a critical condition characterized by the sudden obstruction of pulmonary arteries by a thrombus, often originating from deep vein thrombosis.[12] This obstruction can lead to impaired gas exchange, RV strain, and systemic hemodynamic instability.[13] Key clinical manifestations include dyspnea, pleuritic chest pain, tachypnea, tachycardia, and, less frequently, hemoptysis or syncope. Diagnosis involves a comprehensive assessment using the Wells score,[14] elevated D-dimer levels, and imaging techniques like CT or lung ventilation perfusion (V/Q) scans.[15] Acute PE severity is classified as massive (with hemodynamic instability), submassive (with RV dysfunction), or low-risk. Treatment typically involves anticoagulation, with thrombolysis or surgical intervention considered for severe cases. Adherence to these guidelines and diagnostic approaches is crucial for optimizing treatment outcomes and improving patient survival.[16]

Dataset

The present retrospective study was conducted at Sultan II Abdulhamid Han Training and Research Hospital using data collected between 2017 and 2023; all analyses were performed at the Northwestern University's Machine & Hybrid Intelligence Lab. In all, 207 patients diagnosed with acute PE were included in the study, and all patients underwent CT scanning. Patients diagnosed with acute PE by 1 radiologist, 1 pulmonologist, and 1 cardiologist were included in the study.

Patients were eligible to participate in the study if they had a filling defect in the pulmonary artery or branches on CT, were aged ≥18 years, and had acute PE symptom duration ≤14 days. Patients with stroke or transient ischemic attack, recent (in the previous 3 months) head trauma, major surgery within the previous 7 days, a positive COVID-19 polymerase chain reaction (PCR) test on admission, acute end-stage renal disease, and/or acute end-stage hepatic disease were excluded from the study. Baseline demographic and clinical characteristics of the study cohort were extracted from electronic hospital records (EHR). In addition, biochemical analyses, electrocardiogram readings, and echocardiographic data obtained on admission were collected from the hospital records.

CT Angiography Protocol for Acute PE

CT scans were performed in all patients to diagnose acute PE using a Canon Aquilion 128-Slice CT Scanner.

Patient Preparation For suspected acute PE, immediate imaging was prioritized within 30–60 min after admission. Intravenous access was established with an 18- to 20-gauge cannula in the antecubital fossa.

Imaging Parameters Scans were performed with the patient supine. Parameters included a tube voltage of 120 kV, tube current of 150–300 mAs, and pitch of 0.75–0.85. The images had a pixel matrix of 512×512, pixel spacing of 1 mm×1 mm, slice thickness of 0.5 mm, reconstruction interval of 0.5 mm, and a rotation time of 0.35 s.

Contrast Administration A non-ionic iodinated contrast agent (iohexol) was administered intravenously at a dose of 1 mL/kg at a rate of 4.0–5.0 mL/s, followed by a 30–50 mL saline flush injected at the same rate.

Bolus Tracking and Timing Bolus tracking was used with the region of interest (ROI) in the main pulmonary artery, triggering the scan when attenuation reached 100–120 Hounsfield Units (HU), typically 10–15 s after contrast injection.

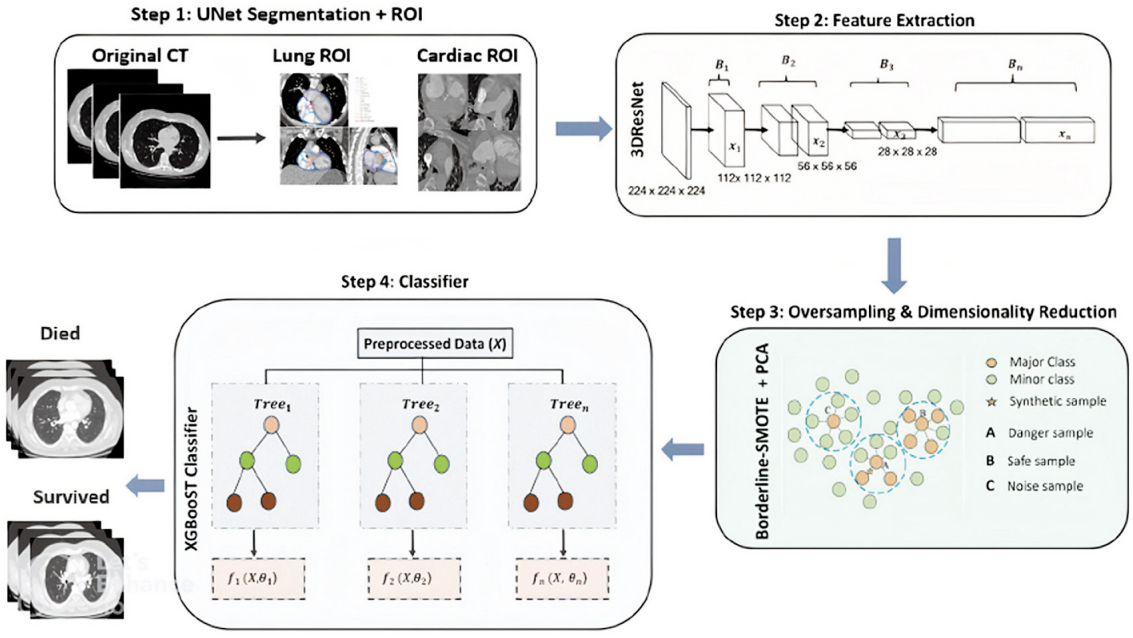


Figure 2. Proposed deep learning model architecture for mortality prediction for pulmonary embolism patients consisting of 4 consecutive steps: (1) localization of approximate lung and cardiac regions of interest (ROIs); (2) feature extraction with deep nets; (3) oversampling and dimensionality reduction; and (4) an optimized classifier. CT, computed tomography; PCA, principal component analysis.

Image Reconstruction Images were reconstructed using a standard or sharp algorithm optimized for pulmonary vessel visualization, generating multiplanar reconstructions in axial, coronal, and sagittal planes.

Radiation Dose Management Dose modulation techniques were used to minimize radiation exposure, adjusting imaging parameters according to patient size.

Summary of the Deep Learning Imaging Model Structure

Our contributions can be summarized as follows:

1. We introduce a novel deep learning-based approach, the mmDL model, that includes several interconnected modules, carefully designed to automatically analyze CT scans. Two representative CT images of lobar and distal PE are shown in **Figure 1**.
2. These modules include U-Net for "roughly" estimating the location of the lungs and heart, a 3-dimensional residual network (3DResNet) for extracting volumetric hierarchical features, principal component analysis (PCA) to reduce feature dimensionality, BorderlineSMOTE (B-SMOTE) to solve class-imbalance problems, and XGBoost to take the learned features and focus on the relationships that are most predictive of outcome.
3. We devised a U-Net segmentor inside the model to determine lung and cardiac regions automatically and to use these as an input to predict 30-day mortality. The aim of separating the cardiac and lung regions was to enable the combination of findings from lobar and distal cases of PE, if needed.
4. Our comprehensive results demonstrate that the model outperforms other baselines, achieving superior performance (area under the curve [AUC]=0.94) while the closest results obtained.

Deep Learning Prognosis Our proposed approach consists of several steps, as shown in **Figure 2**:

- identifying the lung ROI and cardiac ROI
- using a 3DResNet model to extract features
- using PCA to reduce dimensionality
- using B-SMOTE to handle class-imbalance problems
- using a fine-tuned, optimized XGBoost classifier to train and evaluate the model's performance.

3DResNet With a New Convolutional Layer In our study we used a pretrained 3DResNet model, specifically the ResNet18 variant with 18 layers, known for its fine-tuned weights acquired from substantial training data. These pretrained weights enhance performance, particularly with smaller datasets, by expediting convergence. The model structure, adapted from the original pretrained model, follows a sequential design but omits the first and last layers. The first layer, initially intended for 3-channel RGB images, is replaced to accommodate grayscale CT images with a single channel. Likewise, the final fully connected layer, designed for classification, is removed to focus on feature extraction.

We also introduced a new 3-dimensional (3D) convolutional layer to process the 1-channel input, aligning with grayscale CT images and generating a 64-channel feature map. This layer maintains the original first layer's kernel size, stride, and padding parameters. It involves a kernel size of (7,7,7), a stride of (2,2,2), and a padding of (3,3,3) to preserve spatial dimensions after convolution by adding border pixels (**Figure 2**, Step 2).

Oversampling and Feature Selection We used an advanced oversampling technique, B-SMOTE, because we had a class imbalance problem (20% vs. 80% distribution of patients with PE) and classifier performance is subopti-

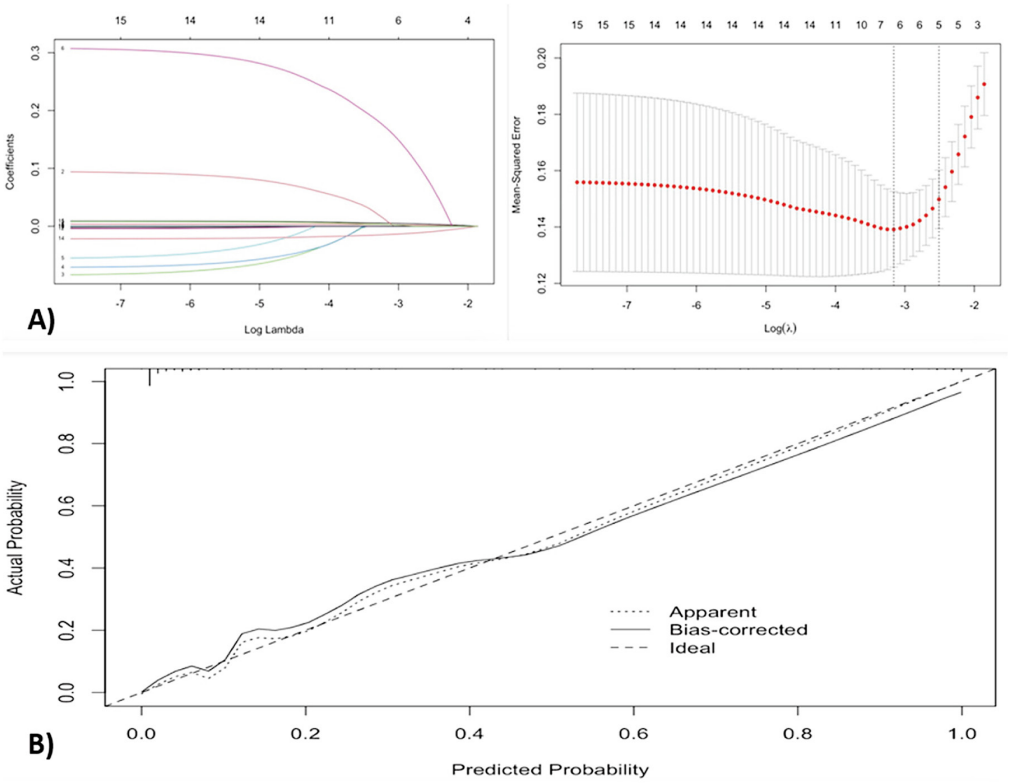


Figure 3. (**A**) LASSO (least absolute shrinkage and selection operator) penalized shrinkage was used to select the most relevant variables for multivariable logistic regression analysis. (**B**) Calibration plot of the multimodal deep learning model.

mal with class imbalance. We applied default parameters, including a sampling strategy of "auto", a k-neighbors value of 5, and an m-neighbors value of 10. For a given minority class sample x_i and its selected neighbor x_{in}, a synthetic sample x_{new} was generated using Eqn 1:

$$x_{new} = x_i + \lambda \times (x_{in} - x_i) \qquad [1]$$

where λ is a random number between 0 and 1. Next, we applied PCA-based dimensionality reduction (feature selection) to our system. PCA is widely used for feature selection, especially after the generation of a large number of features by DL networks. The number of principal components for PCA was determined on the basis of experimentation, with a range of 50–150 components tested. The optimal performance was achieved with 100 components (empirically determined).

Classification With XGBoost The XGBoost classifier was used with the objective set as "binary:logistic", indicating a binary classification problem with logistic regression for probability prediction. Key parameters included a learning rate of 0.1, which balances model training speed and performance, and a maximum tree depth of 3 to limit model complexity and mitigate overfitting. The model was trained with 100 boosting rounds. The scale pos weight parameter, calculated as the ratio of the number of negative cases to the number of positive cases in the training data, was used to give higher importance to the minority class during training. For a given iteration i, the updated equation for the XGBoost classifier Fi(x) can be expressed as follows:

$$F_i(x) = F_i - 1(x) + \eta \times h_i(x) \qquad [2]$$

where $F_i - 1(x)$ is the model at iteration $i-1$, η is the learning rate, and $h_i(x)$ is the new decision tree added at iteration i.

Further Details on Training The DL imaging model and other baselines underwent training for up to 100 epochs, using Sparse Categorical Cross Entropy as the loss function, with the ADAM optimizer set along with a learning rate of 0.0001. The training was conducted on a high-performance GPU server equipped with 1 NVIDIA A100 GPU and 80 GB memory, operating under Debian Linux. We evaluated the performance of each method based on metrics such as accuracy and AUC. We used 5-fold cross-validation during the experiments, ensuring robustness and reliability in our results.

Statistical Analysis

R software version 4.2.2 (R Foundation for Statistical Computing, Vienna, Austria) was used for all statistical analyses. The assumption of a normal distribution was assessed using the Kolmogorov-Smirnov test. Normally and non-normally distributed data are presented as the mean ± SD and median with interquartile range (IQR), respectively. Categorical data are presented as numbers and percentages. Categorical variables were compared using the χ^2 test or Fisher's exact test. Continuous variables were compared between research groups using the Mann-Whitney U test or the independent Student's t-test. To

Table 1. Patient Characteristics According to Mortality Status at 30 Days

	Survivors (n=154)	Non-survivors (n=53)	P value
Demographic variables and vital signs			
Age (years)	69.5 [57.2–79.0]	80.0 [74.0–88.0]	<0.001*
Male sex	63 (40.9)	25 (47.2)	0.526
Hypertension	91 (59.1)	32 (60.4)	0.998
Diabetes	44 (28.6)	14 (26.4)	0.901
History of HF	5 (3.25)	16 (30.2)	<0.001*
COPD	27 (17.5)	12 (22.6)	0.537
CKD	7 (4.55)	1 (1.89)	0.683
History of cancer	21 (13.6)	19 (35.8)	0.001*
Oxygen saturation (%)	92.5 [86.0–96.0]	88.0 [86.0–93.0]	0.004*
Heart rate (beats/min)	89.0 [78.0–102]	105 [88.0–120]	<0.001*
SBP (mmHg)	125 [116–134]	120 [100–130]	0.030*
DBP (mmHg)	75.0 [70.0–80.0]	70.0 [60.0–78.0]	0.005*
PESI score	90.5 [72.2–106]	127 [118–152]	<0.001*
Laboratory results			
D-dimer (ng/mL)	2,700 [1,498–4,000]	2,770 [1,920–4,000]	0.400
Troponin (ng/dL)	30.5 [12.0–106]	56.0 [26.0–114]	0.007*
BNP (pg/mL)	342 [97.8–1,243]	1015 [262–6,352]	0.001*
Creatinine (mg/dL)	1.27 [1.00–2.16]	1.00 [0.82–1.27]	0.003*
ALT (U/L)	19.0 [12.0–30.0]	22.0 [12.0–43.0]	0.119
AST (U/L)	21.0 [16.0–31.0]	31.0 [23.0–63.0]	<0.001*
Glucose (mg/dL)	118 [99.2–157]	153 [126–192]	0.001*
CRP (mg/dL)	40.0 [20.0–97.8]	72.0 [20.0–135]	0.048*
WBC ($\times 10^3/\mu L$)	13.2 [6.00–16.2]	16.0 [6.00–18.0]	0.273
Hemoglobin (g/dL)	13.0 [10.0–14.4]	14.0 [10.0–14.4]	0.358
Platelets ($\times 10^3/\mu L$)	235 [189–296]	269 [181–326]	0.381
Neutrophils ($\times 10^3/\mu L$)	7.11 [4.84–12.6]	6.60 [4.84–10.8]	0.037*
Lymphocytes ($\times 10^3/\mu L$)	1.65 [1.14–2.30]	1.41 [0.73–1.90]	0.020*
pH	7.40 [7.34–7.45]	7.41 [7.33–7.47]	0.843
Lactate	1.60 [1.30–2.40]	2.23 [1.60–2.78]	0.009*
HCO_3 (mmol/L)	24.4 [22.3–27.5]	23.7 [21.0–26.7]	0.264
Echocardiography			
Ejection fraction (%)	60.0 [60.0–60.0]	60.0 [45.0–60.0]	<0.001*
TAPSE (mm)	22.0 [19.0–23.0]	16.0 [14.0–21.0]	<0.001*
RV (mm)	35.5 [32.0–40.0]	35.5 [30.0–41.0]	0.741
RA (mm)	37.0 [25.0–49.0]	47.0 [30.0–49.0]	0.016*
LVIDD (mm)	46.0 [44.0–49.8]	48.0 [44.0–51.0]	0.127
LAAP (mm)	36.0 [34.0–41.0]	41.0 [36.0–45.0]	<0.001*
SPAP (mmHg)	35.0 [25.0–45.0]	35.0 [28.0–50.0]	0.400
Follow-up			
ICU hospitalization (day)	0.00 [0.00–2.75]	4.00 [1.00–9.00]	<0.001*
Sum-up hospitalization (day)	8.00 [6.00–10.0]	10.0 [4.00–20.0]	0.164

*Represents statistically significant values (P<0.05). Unless indicated otherwise, data are given as the median [interquartile range] or n (%). ALT, alanine aminotransferase; AST, aspartate aminotransferase; BNP, B-type natriuretic peptide; CKD, chronic kidney disease; COPD, chronic obstructive pulmonary disease; CRP, C-reactive protein; DBP, diastolic blood pressure; HF, heart failure; ICU, intensive care unit; LAAP, left atrium anterior posterior dimension; LVIDD, left ventricular internal diastolic dimension; PESI, pulmonary artery severity index; RA, right atrium; RV, right ventricle; SBP, systolic blood pressure; SPAP, systolic pulmonary artery pressure; TAPSE, tricuspid annular plane systolic excursion; WBC, white blood cells.

avoid overfitting, LASSO (least absolute shrinkage and selection operator) penalized shrinkage with an optimal lambda value was used for variable selection to create a multivariable model (**Figure 3A**). Logistic regression analysis was conducted with variables selected from the LASSO penalized regression to predict the 30-day mortality of PE patients in the logistic model. Another model was created based on the $\log_{10}$(odds) of the predicted values obtained from the DL model, and this model was used to predict the 30-day mortality of patients with PE using only CT scans without EHR data. We created a mixed model by combining the DL and logistic models, which we termed the mmDL model. We used receiver operating characteristic (ROC) curves to compare the discriminative abilities

Table 2. Logistic Regression Analysis for Predicting 30-Day Mortality			
	OR	95% CI	P value
Age	10.136	3.870–26.546	<0.001
Heart rate	2.855	1.348–6.048	0.0062
BNP	1.159	1.024–1.312	0.0187
TAPSE	0.253	0.121–0.527	0.0002
Cancer	13.111	4.129–41.630	<0.001

CI, confidence interval; OR, odds ratio. Other abbreviations as in Table 1.

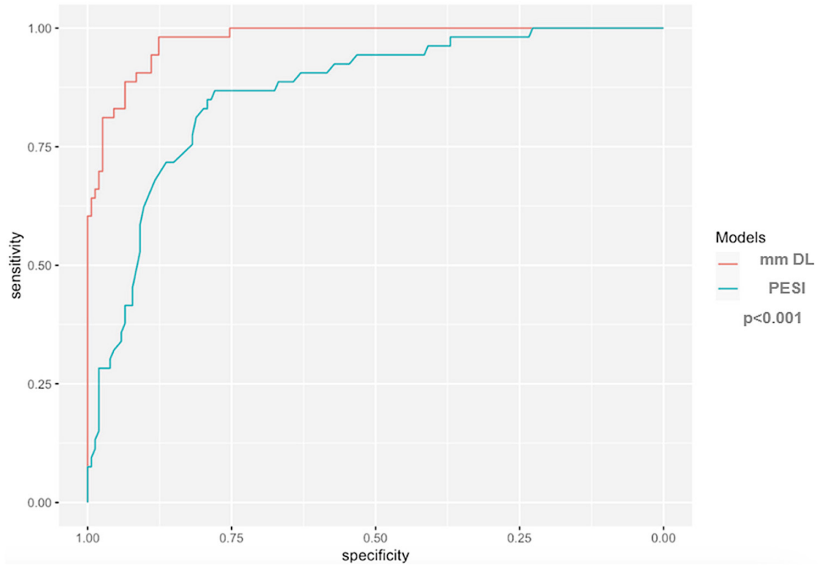


Figure 4. Comparison of the performance of the multimodal deep learning (mmDL) model with Pulmonary Embolism Severity Index (PESI) scoring in predicting short-term mortality in pulmonary embolism patients.

between the models, namely the logistic, DL, mmDL, and PESI models; in the latter, PESI was used as independent predictor of 30-day mortality. A risk scoring nomogram was created based on the mmDL model, and $\log_{10}$(odds) values of the risk of mortality obtained from the DL model were input as the predicted probability for ease of use. Bootstrap with 300 repetitions was used for internal validation of the mmDL model and a calibration plot was created to assess the reproducibility of the model in the new datasets (**Figure 3B**). The level of significance for the results was set at 2-sided P<0.05.

Results

Patient Characteristics

This retrospective study included 207 PE patients. During the 1-month follow-up, 53 patients died. The study cohort was divided into 2 groups, survivors and non-survivors, based on short-term (0–30 days) mortality status.

Table 1 presents the characteristics of the 2 groups. Those in the non-survivor group were older and were more likely to have heart failure and a history of cancer. Of the examination findings, low oxygen saturation, tachycardia, systolic and diastolic hypotension, and high PESI scores were statistically significant in the non-survivor group. Laboratory values, such as elevated troponin, B-type natriuretic peptide (BNP), creatinine, glucose, aspartate aminotransferase, C-reactive protein, and lactate, as well as low neutrophil and lymphocyte levels, were statistically significant in the non-survivor group. Echocardiographic examinations revealed that a low ejection fraction, low tricuspid annular plane systolic excursion (TAPSE), and enlargement of the right and left atria were associated with short-term mortality. Admission to the intensive care unit was more frequently observed in the non-survivor group.

Table 2 presents the results of logistic regression for predicting 30-day mortality. Age (odds ratio [OR] 10.136; 95% confidence interval [CI] 3.870–26.546; P<0.001), heart rate (OR 2.855; 95% CI 1.348–6.048; P=0.0062), BNP (OR 1.159; 95% CI 1.024–1.312; P=0.0187), TAPSE (OR 0.253; 95% CI 0.121–0.527; P=0.0002), and cancer (OR 13.111; 95% CI 4.129–41.630; P<0.001) were found to be significantly related to short-term mortality.

Our DL method was to assess the efficacy of these models in predicting 30-day mortality in PE patients using either lung ROI or cardiac ROI inputs. We used 5-fold cross-validation during the experiments, ensuring the robustness and reliability in our results. The proposed model has high accuracy, suggesting it is highly effective at making correct mortality predictions. The AUC (0.94; P<0.001) indicates that our model has superior ability to distinguish between the classes. These results underscore the potential of our proposed model for improving mortality prediction in PE patients. We then developed a new

Advance Publication

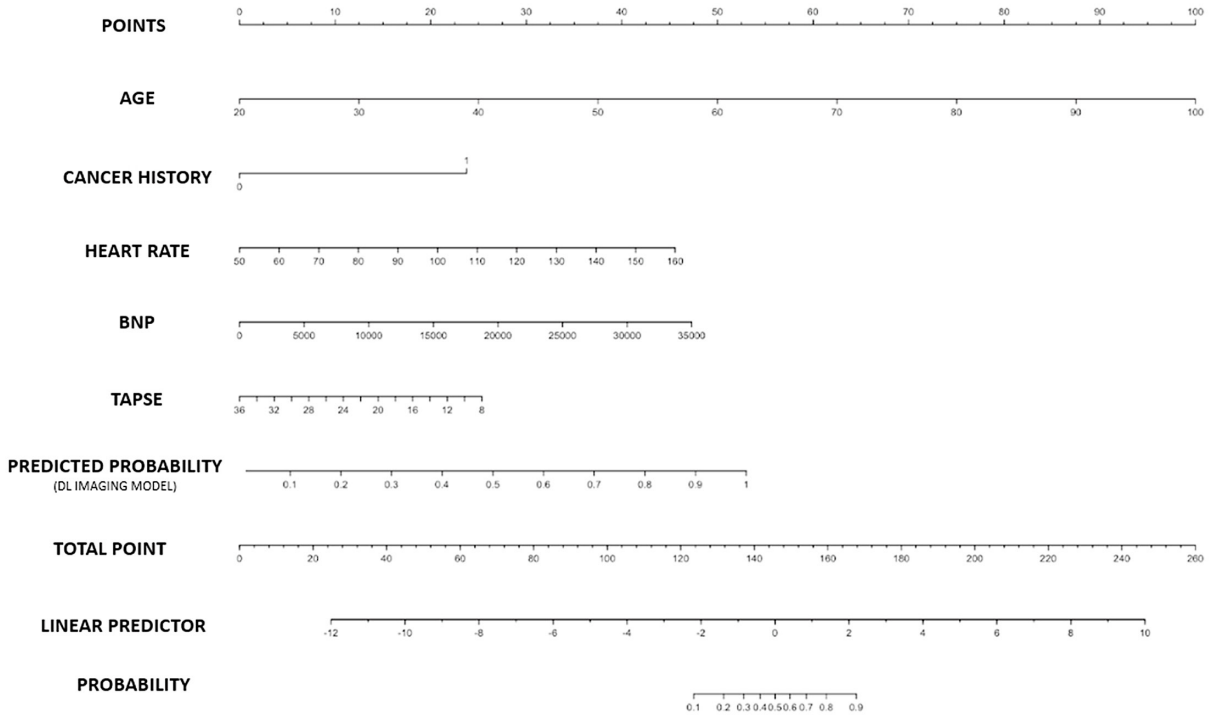


Figure 5. Scoring chart for the multimodal deep learning (mmDL) model. BNP, B-type natriuretic peptide; DL, deep learning; TAPSE, tricuspid annular plane systolic excursion.

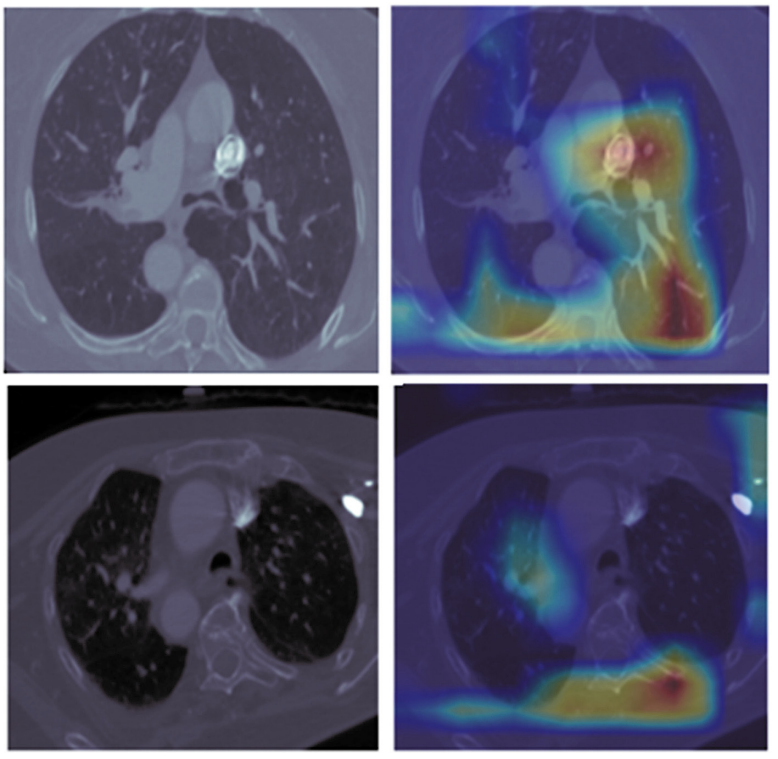


Figure 6. GradCAM visualizations generated from 3DResNet showing model focus on different regions across input images.

score model by combining the independent predictors of short-term mortality specified in **Table 2**, EHR data, and the DL model. The ROC analysis demonstrated an AUC of 0.976 (P<0.001) for the mmDL model score and an AUC of 0.865 (P<0.001) for the PESI score. Both scores were found to be statistically significant in predicting short-term mortality. However, the mmDL model was found to be superior to the PESI score (P<0.001; **Figure 4**). An mmDL model scoring chart was created (**Figure 5**). In our model with 5 different parameters and predicted probability from the DL imaging model, each parameter is evaluated in patients, with results marked on the chart and the corresponding points for each of the parameters then summed. The summed score is marked on the "Total Points" line, with the corresponding "Probability" on the row below indicating the short-term (0–30 days) mortality risk.

We further analyzed our model's performance using GradCAM (M3D-Cam[43]) to visualize the regions of focus identified by the 3DResNet network. As shown in the top panels of **Figure 6**, the model focuses on the cardiac and lung regions, reflecting its attention on areas relevant to the task. In contrast, the bottom panels in **Figure 6** highlight a less optimal focus, with some attention on the cardiac region but a degree of misalignment in other feature areas. It is important to note that the pre-trained 3DResNet network was not trained on domain-specific data, contributing to the probability of obtaining a suboptimal Grad-CAM. Despite this, they still offer insights into the model's behavior and may highlight areas where further refinement is necessary.

Discussion

In this paper we introduce a new mmDL model, tailored for the prognostication of PE, a critical cardiovascular ailment with high mortality rates. This model has been demonstrated to be significantly superior to the PESI score recommended by current international guidelines for prognosis analysis.

The PESI score is a widely used tool to predict 30-day mortality rates in patients with PE. It evaluates patients based on their comorbidities and vital signs at hospital admission and is recommended by the 2019 Acute Pulmonary Embolism guidelines of the European Society of Cardiology. The PESI scoring system assesses a total of 11 clinical parameters, including heart rate, systolic blood pressure, oxygen saturation on room air, respiratory rate, and level of consciousness.[9,11] The sensitivity of the PESI score in predicting 30-day mortality in patients with PE is approximately 80–90%, whereas its specificity ranges from 40% to 60%.[17] This means that it may classify some patients as high risk who are not actually at high risk of mortality. Therefore, there is an unmet need for the development of better models with higher sensitivity and specificity that can distinguish between low- and high-risk patients. We have demonstrated that our mmDL model is significantly more successful at distinguishing between patients at low and high risk of mortality than the PESI score.

Accurate stratification of acute PE patients as either low or high risk allows clinicians to personalize treatment strategies, as well as enabling those at high risk to receive more aggressive therapeutic interventions, such as thrombolysis, embolectomy and extracorporeal membrane oxygenation (ECMO). Thrombolytic therapy is typically indicated for individuals experiencing severe or massive PE. Research indicates that thrombolytic agents can dissolve blood clots more quickly than the other anticoagulants and potentially lower the mortality risk associated with PE.[18,19] Embolectomy is advised for patients with high-risk PE who have absolute contraindications to thrombolytics, have experienced treatment failure, or are in cardiogenic shock that could lead to death before thrombolytic therapy can be administered. Surgical embolectomy is often regarded as the primary intervention for patients with a thrombus located in the heart.[20,21]

Another therapeutic option is ECMO, which has been shown to significantly lower mortality rates. ECMO is effective when used in conjunction with any of the aforementioned treatments, yielding favorable survival rates and low complication risks. ECMO provides comprehensive hemodynamic support with an output of 5–6 L while integrating an oxygenator to assist with oxygenation and ventilation. Importantly, by bypassing the pulmonary circulation, ECMO reduces RV preload and diminishes RV distension without affecting pulmonary artery pressure, thereby contributing to a significant reduction in mortality.[22,23] In addition to these treatments, inferior vena cava filters may be used in cases of recurrent embolism or when anticoagulation is absolutely contraindicated. The PREPIC trial demonstrated a short-term benefit and long-term efficacy of inferior vena cava filters in preventing PE recurrence.[24] Conversely, low-risk patients can often be managed with less intensive approaches, such as anticoagulation therapy alone, thus minimizing exposure to potential complications associated with more invasive therapies. This differentiated approach not only enhances patient safety but also improves resource utilization and overall healthcare efficiency. Furthermore, appropriate risk assessment facilitates timely and appropriate discharge planning and follow-up, further contributing to improved long-term outcomes and quality of life for PE patients.[25,26]

Deaths due to PE are often caused by RV dysfunction and malignant arrhythmias. Various studies have indicated that certain CT findings can serve as reference markers for RV dysfunction. A short-axis RV/left ventricular ratio >1 on CT is correlated with increased afterload induced by acute PE on ventricular function.[27] Other indicators of RV dysfunction include coronary sinus dilatation (>9 mm), increased pulmonary artery diameter, clot burden, and interventricular septal flattening or curvature.[28–30] The DL model we developed based on CT imaging predicted short-term mortality in PE patients in a statistically significant manner, consistent with information from the existing literature.

Numerous previous studies have shown that DL-based prognostic models have superior predictive performance.[31] The model we developed accurately predicts short-term mortality in acute PE patients. Several factors contribute to the success of our model. First, we used BorderlineSMOTE to address the dataset's imbalance, generating synthetic samples for the minority class. This balancing technique proved effective in improving model generalization.[32] In addition, we incorporated PCA to reduce dimensionality, enhancing feature representation. This integration, alongside the 3DResNet architecture and XGBoost algorithm, created a powerful combination.[33] ResNet excels at feature extraction and learning representations from images,[34] whereas XGBoost, renowned for its ability to handle imbalanced datasets, plays a pivotal role. XGBoost, in combination with BorderlineSMOTE, focuses on the

minority class, effectively addressing data imbalance by giving greater attention to challenging instances. This boosting approach enabled our model to learn from its mistakes and refine its predictions, which is particularly vital in imbalanced medical datasets. Validated on 207 CT scans, the DL imaging model achieved remarkable accuracy rates above 94%.

Of the clinical and demographic data used to develop the mmDL model, being elderly, having tachycardia, history of cancer, low TAPSE, and high BNP were found to be independent predictors of short-term mortality in acute PE patients. Acute PE seems very common and with greater mortality in elderly people. Additional comorbidities can delay the diagnosis of acute PE, thus increasing the mortality rate due to delays in patients receiving the correct treatment, and increasing the risk of mortality themselves.[35,36] In epidemiological studies, although the 0–30-day mortality rate due to acute PE in the general population was around 5%, another study among those aged ≥80 years reported that the 30-day mortality was 18.9% among patients with confirmed acute PE.[37,38]

Acute PE is a common and potentially lethal disease in cancer patients. Cancer patients appear to be at higher risk for central acute PE and, as a result, are more likely to have longer hospital stays after diagnosis than those without cancer. Cancer patients have a 4-fold higher risk of acute PE compared with the general population.[39,40] Based on the results of our study, cancer is an independent variable for short-term mortality prediction in acute PE patients.

The prognosis for acute PE patients can be predicted based on hemodynamic status, RV dysfunction, myocardial damage, arrhythmias, and other clinical and routine laboratory tests. Shock and hypotension are major indicators of early mortality risk in acute PE.[41] BNP is released by the heart ventricles in response to ventricular strain. BNP has been proposed as a potentially useful biomarker for the detection of RV dysfunction in acute PE and, as a result, for the prediction of mortality.[42] TAPSE reflects the systolic function of the RV, and TAPSE ≤15 mm after acute PE is associated with an increased risk of early mortality. Tachycardia is another mortality predictor in acute PE patients, especially when a patient's heart rate is higher than 110 beats/min at the time of admission.[43,44] In our study, tachycardia on admission, elevated BNP, reduced TAPSE, and laboratory and imaging findings were significantly associated with short-term mortality in acute PE patients, with all these parameters used to develop our mmDL model, enhancing its predictive power.

Study Limitations

Although our study shows promising results, it does have some limitations that we aim to address in the future. The main limitation of our study was that it was a retrospective single-center study. However, all consecutive patients were included in the analysis. Despite using multivariate analysis to determine independent predictors of in-hospital mortality, there may be some unmeasured confounders. Our study can be integrated into a prospective cohort once it is validated in multicenter studies. Finding the patients who are most at risk of adverse outcomes will ease the clinical workflow and require existing guidelines to be replaced by new ones, likely by DL-powered explainable systems. Getting data from multiple centers is a challenge at the moment due to privacy concerns. Our study could also benefit from more advanced backbone models, such as ViT or, more recently, a Mamba-type of new architecture; however, the data-hungry nature of Transformers (used in this study) should be kept in mind, along with the limited data. One may also ask whether solely designed deep networks (ViT, Mamba, and others) can solve this problem without the need for XGBoost or other separate classifiers. The decision to combine traditional machine learning techniques, such as XGBoost, with DL architecture, like 3DResNet, for classification tasks is a strategic approach that leverages the strengths of both methodologies to achieve superior performance, not only the lack of enough data to attend.

Conclusions

This study developed a new mmDL model that used both CT images and baseline EHR data to predict short-term (0–30 days) mortality in patients with acute PE. The mmDL model significantly outperformed the reference scoring system, the PESI, demonstrating the potential of DL techniques to improve risk stratification and guide clinical decision making in acute PE patients. Beyond surpassing the PESI score, the ability of the mmDL model to identify novel predictive features extracted from CT scans highlights the power of DL to discover previously unknown associations between imaging data and clinical outcomes. This paves the way for further research exploring the integration of DL with traditional clinical data in various medical fields. Although our study presents encouraging results, further validation is required in larger and more diverse patient populations. Moreover, future studies should explore the interpretability of the DL model to understand the underlying mechanisms that contribute to its improved accuracy. Overall, this study offers a promising step towards personalized risk prediction and potentially life-saving interventions in acute PE patients. Further research can refine and translate this approach into routine clinical practice, ultimately improving patient care and outcomes.

Acknowledgment

Not applicable.

Sources of Funding

U.B. is supported by National Institutes of Health grants (R01-CA246704, R01-CA240639, U01-DK127384-02S1, and U01-CA268808).

Disclosures

The authors declare no conflicts of interest.

IRB Information

This study was approved by the Clinical Research Committee of Haydarpaşa Numune Training and Research Hospital, Istanbul, Turkey (No. HNEAH-KAEK 2023/17).

Data Availability

The datasets generated and/or analyzed in this study are available from the corresponding author upon reasonable request.

References

1. Mazzolai L, Aboyans V, Ageno W, Agnelli G, Alatri A, Bauersachs R, et al. Diagnosis and management of acute deep vein thrombosis: A joint consensus document from the European Society of Cardiology working groups of aorta and peripheral vascular diseases and pulmonary circulation and right ventricular func-

Advance Publication

tion. *Eur Heart J* 2018; **39:** 4208–4218.
2. JCS Joint Working Group. Guidelines for the diagnosis, treatment and prevention of pulmonary thromboembolism and deep vein thrombosis (JCS 2009): Digest version. *Circ J* 2011; **75:** 1258–1281.
3. Raskob GE, Angchaisuksiri P, Blanco AN, Buller H, Gallus A, Hunt BJ, et al. Thrombosis: A major contributor to global disease burden. *Arterioscler Thromb Vasc Biol* 2014; **34:** 2363–2371.
4. Farmakis I, Valerio L, Mavromanoli A, Bikdeli B, Connors J, Giannakoulas G, et al. Mortality related to pulmonary embolism in the United States before and during the COVID-19 pandemic: An analysis of the CDC Multiple Cause of Death database. *Eur Heart J* 2022; **43**(Suppl 2)**:** ehac544.1869, doi:10.1093/eurheartj/ehac544.1869.
5. Wendelboe AM, Raskob GE. Global burden of thrombosis: Epidemiologic aspects. *Circ Res* 2016; **118:** 1340–1347.
6. Surov A, Akritidou M, Bach AG, Bailis N, Lerche M, Meyer HJ, et al. A new index for the prediction of 30-day mortality in patients with pulmonary embolism: The Pulmonary Embolism Mortality Score (PEMS). *Angiology* 2021; **72:** 787–793.
7. Russell C, Keshavamurthy S, Saha S. Classification and stratification of pulmonary embolisms. *Int J Angiol* 2022; **31:** 162–165.
8. Chatani R, Yamashita Y, Morimoto T, Muraoka N, Shioyama W, Shibata T, et al. Home treatment for active cancer patients with low-risk pulmonary embolism: A predetermined companion report from the ONCO PE Trial. *Circ J* 2024, doi:10.1253/circj.CJ-24-0004.
9. Konstantinides SV, Meyer G, Becattini C, Bueno H, Geersing GJ, Harjola VP, et al. 2019 ESC guidelines for the diagnosis and management of acute pulmonary embolism developed in collaboration with the European Respiratory Society (ERS) The Task Force for the Diagnosis and Management of Acute Pulmonary Embolism of the European Society of Cardiology (ESC). *Eur Heart J* 2020; **41:** 543–603.
10. Goldhaber S, Come P, Lee R, Braunwald E, Parker J, Haire W, et al. Alteplase versus heparin in acute pulmonary embolism: Randomised trial assessing right-ventricular function and pulmonary perfusion. *Lancet* 1993; **341:** 507–511.
11. Sandal A, Korkmaz ET, Aksu F, Köksal D, Selçuk ZT, Demir AU, et al. Performance of Pulmonary Embolism Severity Index in predicting long-term mortality after acute pulmonary embolism. *Anatol J Cardiol* 2021; **25:** 544.
12. Kearon C, Akl EA, Ornelas J, Blaivas A, Jimenez D, Bounameaux H, et al. Antithrombotic therapy for VTE disease: CHEST guideline and expert panel report. *Chest* 2016; **149:** 315–352.
13. Minhas J, Nardelli P, Hassan SM, Al-Naamani N, Harder E, Ash S, et al. Loss of pulmonary vascular volume as a predictor of right ventricular dysfunction and mortality in acute pulmonary embolism. *Circ Cardiovasc Imaging* 2021; **14:** e012347.
14. Shen JH, Chen HL, Chen JR, Xing JL, Gu P, Zhu BF. Comparison of the Wells score with the revised Geneva score for assessing suspected pulmonary embolism: A systematic review and meta-analysis. *J Thromb Thrombolysis* 2016; **41:** 482–492.
15. Wildberger JE, Mahnken AH, Das M, Küttner A, Lell M, Günther RW. CT imaging in acute pulmonary embolism: Diagnostic strategies. *Eur Radiol* 2005; **15:** 919–929.
16. Castillo C, Tapson VF. Right ventricular responses to massive and submassive pulmonary embolism. *Cardiol Clin* 2012; **30:** 233–241.
17. Jiménez D, Aujesky D, Moores L, Gómez V, Lobo JL, Uresandi F, et al. Simplification of the pulmonary embolism severity index for prognostication in patients with acute symptomatic pulmonary embolism. *Arch Intern Med* 2010; **170:** 1383–1389.
18. Gotkowski K, Gonzalez C, Bucher A, Mukhopadhyay A. M3d-CAM: A PyTorch library to generate 3D attention maps for medical deep learning. *Bildverarb Med* 2021, doi:10.1007/978-3-658-33198-6_52.
19. Zuo Z, Yue J, Dong BR, Wu T, Liu GJ, Hao Q. Thrombolytic therapy for pulmonary embolism. *Cochrane Database Syst Rev* 2021; **4:** CD004437.
20. Konstantinides S, Tiede N, Geibel A, Olschewski M, Just H, Kasper W. Comparison of alteplase versus heparin for resolution of major pulmonary embolism. *Am J Cardiol* 1998; **82:** 966–970.
21. Bloomer TL, El-Hayek GE, McDaniel MC, Sandvall BC, Liberman HA, Devireddy CM, et al. Safety of catheter-directed thrombolysis for massive and submassive pulmonary embolism: Results of a multicenter registry and meta-analysis. *Catheter Cardiovasc Interv* 2017; **89:** 754–760.
22. Maron BA, Leopold JA. Emerging concepts in the molecular basis of pulmonary arterial hypertension: Part II: Neurohormonal signaling contributes to the pulmonary vascular and right ventricular pathophenotype of pulmonary arterial hypertension. *Circulation* 2015; **131:** 2079–2091.
23. Yusuff HO, Zochios V, Vuylsteke A. Extracorporeal membrane oxygenation in acute massive pulmonary embolism: A systematic review. *Perfusion* 2015; **30:** 611–616.
24. Malhotra A, Kishore S, Trost D, Madoff DC, Winokur RS. Inferior vena cava filters and prevention of recurrent pulmonary embolism. *Semin Intervent Radiol* 2018; **35:** 105–107.
25. Becattini C, Agnelli G. Risk stratification and management of acute pulmonary embolism. *Hematology Am Soc Hematol Educ Program* 2016; **2016:** 404–412, doi:10.1182/asheducation-2016.1.404.
26. Tice C, Seigerman M, Fiorilli P, Pugliese SC, Khandhar S, Giri J, et al. Management of acute pulmonary embolism. *Curr Cardiovasc Risk Rep* 2020; **14:** 24.
27. Aribas A, Keskin S, Akilli H, Kayrak M, Erdogan HI, Guler I, et al. The use of axial diameters and CT obstruction scores for determining echocardiographic right ventricular dysfunction in patients with acute pulmonary embolism. *Jpn J Radiol* 2014; **32:** 451–460.
28. Lyhne MD, Kline JA, Nielsen-Kudsk JE, Andersen A. Pulmonary vasodilation in acute pulmonary embolism: A systematic review. *Pulm Circ* 2020; **10:** 2045894019899775.
29. Cozzi D, Moroni C, Cavigli E, Bindi A, Caviglioli C, Nazerian P, et al. Prognostic value of CT pulmonary angiography parameters in acute pulmonary embolism. *Radiol Med* 2021; **126:** 1030–1036.
30. Kang DK, Thilo C, Schoepf UJ, Barraza JM, Nance JW, Bastarrika G, et al. CT signs of right ventricular dysfunction: Prognostic role in acute pulmonary embolism. *JACC Cardiovasc Imaging* 2011; **4:** 841–849.
31. Tang M, Gao L, He B, Yang Y. Machine learning-based prognostic prediction models of non-metastatic colon cancer: Analyses based on surveillance, epidemiology and end results database and a Chinese cohort. *Cancer Manag Res* 2022; **14:** 25–35.
32. Nguyen HM, Cooper EW, Kamei K. Borderline over-sampling for imbalanced data classification. *Int J Knowl Eng Soft Data Paradigms* 2011; **3:** 4–21.
33. Ali ZA, Abduljabbar ZH, Taher HA, Sallow AB, Almufti SM. Exploring the power of eXtreme gradient boosting algorithm in machine learning: A review. *AJNU* 2023; **12:** 320–334.
34. Xu W, Fu YL, Zhu D. ResNet and its application to medical image processing: Research progress and challenges. *Comput Methods Programs Biomed* 2023; **240:** 107660.
35. Siccama R, Janssen K, Verheijden N, Oudega R, Bax L, van Delden J, et al. Systematic review: Diagnostic accuracy of clinical decision rules for venous thromboembolism in elderly. *Ageing Res Rev* 2011; **10:** 304–313.
36. Robert-Ebadi H, Righini M. Diagnosis and management of pulmonary embolism in the elderly. *Eur J Intern Med* 2014; **25:** 343–349.
37. Elias A, Mallett S, Daoud-Elias M, Poggi JN, Clarke M. Prognostic models in acute pulmonary embolism: A systematic review and meta-analysis. *BMJ Open* 2016; **6:** e010324.
38. Castelli R, Bergamaschini L, Sailis P, Pantaleo G, Porro F. The impact of an aging population on the diagnosis of pulmonary embolism: Comparison of young and elderly patients. *Clin Appl Thromb Hemost* 2009; **15:** 65–72.
39. Barco S, Valerio L, Ageno W, Cohen AT, Goldhaber SZ, Hunt BJ, et al. Age-sex specific pulmonary embolism-related mortality in the USA and Canada, 2000–18: An analysis of the WHO Mortality Database and of the CDC Multiple Cause of Death database. *Lancet Respir Med* 2021; **9:** 33–42.
40. Poenou G, Dumitru Dumitru T, Lafaie L, Mismetti V, Ayoub E, Duvillard C, et al. Pulmonary embolism in the cancer associated thrombosis landscape. *J Clin Med* 2022; **11:** 5650.
41. Ergan B, Ergün R, Çalışkan T, Aydın K, Tokur ME, Savran Y, et al. Mortality related risk factors in high-risk pulmonary embolism in the ICU. *Can Respir J* 2016; **2016:** 2432808.
42. Coutance G, Le Page O, Lo T, Hamon M. Prognostic value of brain natriuretic peptide in acute pulmonary embolism. *Critical Care* 2008; **12:** R109.
43. Hobohm L, Becattini C, Ebner M, Lerchbaumer MH, Casazza F, Hasenfuß G, et al. Definition of tachycardia for risk stratification of pulmonary embolism. *Eur J Intern Med* 2020; **82:** 76–82.
44. Oh JK, Park JH. Role of echocardiography in acute pulmonary embolism. *Korean J Intern Med* 2023; **38:** 456.